optica

7 μm, ultrafast, sub-millijoule-level mid-infrared optical parametric chirped pulse amplifier pumped at 2 μm

D. Sanchez,[1,*] M. Hemmer,[1,5] M. Baudisch,[1] S. L. Cousin,[1] K. Zawilski,[2] P. Schunemann,[2] O. Chalus,[3] C. Simon-Boisson,[3] and J. Biegert[1,4]

[1]ICFO-Institut de Ciencies Fotoniques, The Barcelona Institute of Science and Technology, 08860 Castelldefels (Barcelona), Spain
[2]BAE Systems, MER15-1813, P.O. Box 868, Nashua, New Hampshire 03061, USA
[3]THALES Optronique S.A.S., Laser Solutions Unit, 2 avenue Gay-Lussac, 78995 Elancourt Cedex, France
[4]ICREA-Institució Catalana de Recerca i Estudis Avançats, 08010 Barcelona, Spain
[5]Current address: Center for Free-Electron Laser Science, Deutsches Elektronen Synchrotron (DESY), Hamburg, Germany
*Corresponding author: daniel.sanchez@icfo.eu

Received 20 October 2015; revised 14 December 2015; accepted 15 December 2015 (Doc. ID 252325); published 5 February 2016

We present a novel all-fiber pumped optical parametric chirped pulse amplifier (OPCPA) architecture to generate self-carrier-to-envelope-phase stable, sub-eight-optical-cycle duration pulses at 7 μm wavelength approaching millijoule-level pulse energy at 100 Hz repetition rate. The system yields a peak power of 1.1 GW and, if focused to the diffraction limit, would reach a peak intensity of 7×10^{14} W/cm^2. The OPCPA is pumped by a 2 μm Ho:YLF chirped pulse amplifier to leverage the highly efficient and broadband response of the nonlinear crystal ZGP. The 7 μm seed at 100 MHz is generated via difference frequency generation from an Er:Tm:Ho multi-arm fiber frequency comb, and a fraction of its output optically injects the Ho:YLF amplifier. While the pulse bandwidth at 7 μm is perfectly suited for nonlinear and spectroscopic applications, current parameters offer, for the first time, to the best of our knowledge, the possibility to explore strong-field physics in an entirely new wavelength range with a ponderomotive force 77 times larger than from an 800 nm source. The overall OPCPA system is very compact and provides a new tool for investigations directly in the molecular fingerprint region of the electro-magnetic spectrum or to drive high harmonic generation to produce fully coherent x-rays in the multi-kiloelectron-volt range and possibly zeptosecond temporal waveforms.

OCIS codes: (140.3070) Infrared and far-infrared lasers; (190.4970) Parametric oscillators and amplifiers; (320.7090) Ultrafast lasers.

http://dx.doi.org/10.1364/OPTICA.3.000147

The development of coherent light sources with emission in the mid-infrared (mid-IR) is currently undergoing a remarkable revolution. The mid-IR spectral range has always been of tremendous interest, mainly to spectroscopists, due to the ability of mid-IR light to access rotational and vibrational resonances of molecules, which give rise to superb sensitivity upon optical probing [1–3]. Previously, high energy resolution was achieved with narrow-band lasers or parametric sources, but the advent of frequency comb sources has revolutionized spectroscopy by providing high energy resolution within the frequency comb structure of the spectrum and at the same time broadband coverage and short pulse duration [4–6]. Such carrier-to-envelope-phase (CEP) controlled light waveforms, when achieved at ultrahigh intensity, give rise to extreme effects such as the generation of isolated attosecond pulses in the vacuum to extreme ultraviolet range (XUV) [7]. Motivated largely by the vast potential of attosecond science, the development of ultraintense few-cycle and CEP-stable sources has intensified [8], and it was recognized that coherent soft x-ray radiation could be generated when driving high harmonic generation (HHG) with long wavelength sources [9–11]. Recently, based on this concept, the highest waveform controlled soft x-ray flux [12] and isolated attosecond pulse emission at 300 eV [13] was demonstrated via HHG from a 1850 nm, sub-two-cycle source [14]. Within strong-field physics, long wavelength scaling may lead to further interesting physics such as the direct reshaping of the carrier field [15], scaling of quantum path dynamics [16], the breakdown of the dipole approximation [17], or direct laser acceleration [18]. The experimental development of long wavelength light sources therefore holds great promise in many fields of science and will lead to numerous applications beyond strong-field physics and attosecond science.

Here, we present, to the best of our knowledge, the first mid-IR optical parametric chirped pulse amplifier (OPCPA) operating at a center wavelength of 7 μm with output parameters suitable already for strong-field experiments. It is also, to our knowledge, the first demonstration of OPCPA using a 2 μm laser pump source, which enables the use of nonoxide nonlinear crystals with typically limited transparency at 1 μm wavelength. This new OPCPA system is all-optically synchronized and generates 0.55 mJ energy, CEP-stable optical pulses. The pulses support

a sub-four-cycle pulse duration and are currently compressed to fewer than eight optical cycles due to uncompensated higher-order phase from the grating compressor, which will be addressed in the future.

A schematic representation of the OPCPA is shown in Fig. 1 and follows the previously proven concept of our 3 μm OPCPA system [19]. The front-end of the system, which seeds both the pump and optical parametric amplifier (OPA) stages, is a multi-color all-fiber laser (Menlo Systems GmbH) [20]. The seeder is based on a mode-locked Er:fiber oscillator and power amplifier, which deliver 1.55 μm wavelength, nanojoule-level pulses at a repetition rate of 100 MHz. The output is split into two arms, the first of which is compressed in fiber to 72 fs with 3 nJ pulse energy. The second output is coupled into a highly nonlinear fiber where the spectrum is broadened to an optical octave via supercontinuum generation. The portion of the broadened spectrum around 2 μm is subsequently split into two arms. The first is used to seed a chain of broadband Tm:Ho fiber amplifiers and delivers 3 nJ energy pulses centered at 2040 nm, which we compress in free space to 130 fs. The second arm is spectrally narrowed to 1.5 nm before seeding a chain of Tm:Ho fiber amplifiers. At the output we obtain 4 nJ, few picosecond pulses.

The mid-IR seed for the OPA chain is generated through difference frequency generation (DFG) of the femtosecond outputs of the fiber laser. Seed generation using DFG was demonstrated to generate large bandwidths in the mid-IR [21], and furthermore, if the input pulses for the DFG originate from a common oscillator, the output will be intrinsically CEP stable [22,23]. Passive CEP stabilization has proven to be robust and reduces the overall complexity of the laser system [24]. We chose the nonlinear crystal $CdSiP_2$ (CSP) as the generation medium due to its unique combination of a high effective nonlinear coefficient ($d_{eff} \sim 84.5$ pm/V), broad phase-matching characteristics in the mid-IR, and a wide transmission window [25]. Using an AR-coated 1.5 mm thick CSP crystal (BAE Systems), the DFG stage produces CEP-stable optical pulses with up to 150 pJ of energy at 100 MHz [26]. The generated spectrum, which is shown as the gray line in Fig. 2, is centered around 6.5 μm and spans the range between 5.5 and 8 μm.

The pump laser is a central component of an OPCPA as it largely determines the performance of the overall system. Currently, the majority of high-intensity mid-IR sources rely on parametric amplifiers pumped by laser systems operating at 1 μm [19,27,28]. However, extending the operating wavelength of OPCPA to longer wavelengths has so far been hindered by an increasingly unfavorable pump-to-idler photon ratio as well as a scarcity of nonlinear crystals with suitable optical and mechanical properties or transparency [29]. Scaling the pump laser to longer wavelengths circumvents these obstacles and has recently been achieved with pump laser systems based on Ho-doped gain media delivering high energy, femtosecond [30] and picosecond [31,32] pulses around 2 μm, suitable for pumping OPAs.

The pump laser of the OPCPA described in this work relies on chirped pulse amplification (CPA) using Ho:YLF as the gain medium [31]. The CPA line is seeded with the narrow-band, 2 μm pulses from the fiber front-end. The few picosecond 2 μm pulses are temporally stretched using a chirped volume Bragg grating (CVBG; OptiGrate Corp.) to a measured duration of 170 ps, suitable for seeding the high gain amplifiers without risk of optical damage. Upon stretching, the pulses are picked at 100 Hz repetition rate and directed toward a Ho:YLF ring regenerative amplifier (RA). Injection and ejection from the cavity are achieved using a rubidium titanyle phosphate (RTP) Pockels cell operated at half-wave voltage. The nanojoule seed pulses are amplified to 4 mJ in the RA and then sent to a single-pass, cryogenically cooled

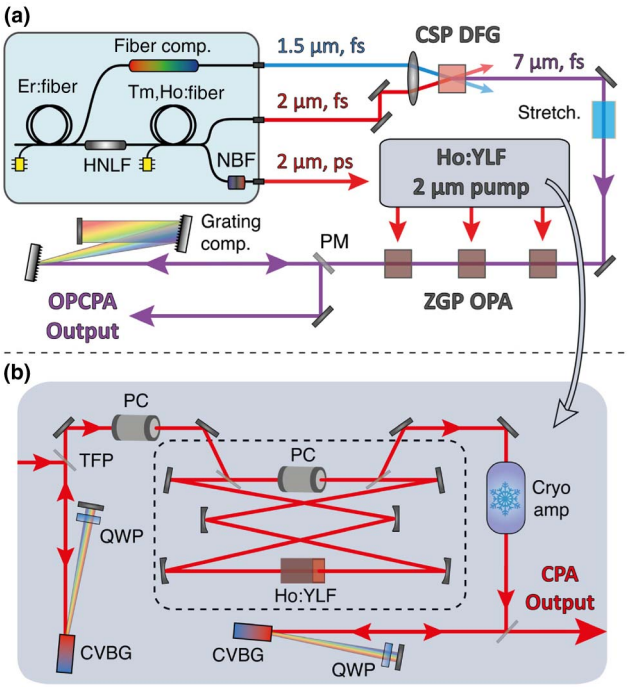

Fig. 1. (a) Layout of the OPCPA concept featuring an all-fiber seeder, a DFG stage, a 2 μm Ho:YLF pump laser, a chain of three consecutive ZGP OPAs, and a reflective grating-based compressor. HNLF, highly nonlinear fiber; NBF, narrow-bandwidth filter; Stretch., stretcher; PM, pick-off mirror; Comp., compressor. (b) Layout of the Ho:YLF CPA featuring a CVBG stretcher, a pulse picker, a ring regenerative amplifier, a single-pass cryogenically cooled booster amplifier, and a CVBG compressor. QWP, quarter-wave plate; CVBG, chirped volume Bragg grating; PC, Pockels cell; TFP, thin-film polarizer.

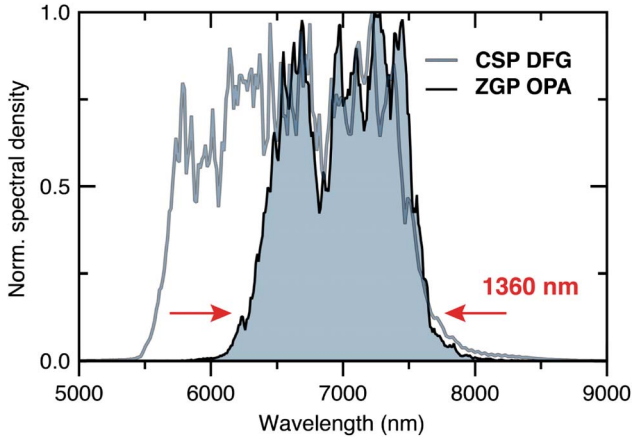

Fig. 2. Spectrum of the mid-IR pulses amplified in the ZGP OPAs (black line, shaded) measured using a scanning monochromator and seed spectrum from the CSP DFG stage (gray line) measured with a Fourier transform infrared spectrometer. The spectral width of the OPCPA output at the 13.5% point is 1360 nm—corresponding to the 85 fs transform limit.

Ho:YLF [33] amplifier. Both the RA and single-pass amplifier are pumped by a CW Tm:fiber laser operating at a wavelength of 1940 nm. At the output of the CPA we measure 40 mJ energy with power fluctuations of less than 0.8% rms and peak-to-peak fluctuations of less than 3% over half a million shots. The compressor is based on a CVBG (OptiGrate Corp.), with a 25 mm × 27 mm aperture. The compressor has an overall efficiency of 85% and is used to temporally compress the output to a measured duration of 11 ps.

The temporal seed stretch factor, which determines the pump-to-seed-pulse duration ratio, is an important design aspect of an OPCPA since it has a large impact on efficiency, amplifiable bandwidth, and superfluorescence generation. There is a trade-off, since in general one-to-one matching of the pump and seed pulse durations leads to a greater efficiency, while a shorter seed pulse leads to broader amplification bandwidths. We used a nonlinear wave propagation code [34] to numerically simulate the DFG and OPA processes in order to choose the stretch factor for the seed. Our simulations suggest that a seed pulse duration of 6 ps together with an 11 ps pump pulse permits amplifying sufficient bandwidth to support a sub-100-fs pulse; note that one optical cycle at 7 μm equals 23 fs. We chose bulk BaF_2 for stretching due to its low Fresnel losses and high GVD in the mid-IR (700 fs^2/mm at 6.5 μm). According to our calculations, the mid-IR seed is stretched to 6 ps after propagating through 12 cm of BaF_2.

The stretched, picojoule-level seed pulses are amplified in a chain of three consecutive noncollinear OPA stages. Due to the large bandwidths and high intensities involved, the nonlinear crystal for the amplifiers needs to be chosen carefully. The use of a 2 μm pump laser allows us to use the highly nonlinear crystal $ZnGeP_2$ (ZGP) ($d_{eff} \sim 75$ pm/V), which for transparency reasons cannot be pumped at a wavelength shorter than 2 μm [29]. The first parametric amplification stage consists of a 5 mm AR-coated ZGP crystal (BAE Systems). Using approximately 200 μJ of pump energy, focused to an intensity of 20 GW/cm^2, and seeding with 100 pJ, the first amplifier exhibits a gain of $\sim 10^4$, yielding 2 μJ of energy in the mid-IR. An identical 5 mm ZGP crystal is used in the second amplification stage, which is pumped with 4 mJ of energy and produces 100 μJ pulses. Finally, the output of the second OPA stage is collimated and loosely focused into the third OPA, which consists of a 3 mm ZGP crystal and is pumped with 8 mJ of energy. This last amplification stage boosts the mid-IR energy to 0.55 mJ. By blocking the seed of the OPA chain we were able to establish an upper limit of superfluorescence contributing to a parametric background of maximally 5%.

The amplified spectrum at the output of the OPCPA is shown in Fig. 2 and was measured using a scanning monochromator equipped with a liquid N_2 cooled mercury cadmium telluride (MCT) detector. The spectrum is centered at 7 μm with a bandwidth of 1360 nm at $1/e^2$, which supports a 85 fs pulse duration (sub-four cycles). Considering that the amplification is ultrabroadband, the measured energy conversion efficiency of 18% into signal plus idler in the last OPA stage is excellent. After amplification, for a first test of compressibility, the mid-IR pulses are directed toward a Martinez-style compressor consisting of a reflective Al-coated diffraction grating with 150 l/mm and an uncoated CaF_2 lens. The total energy throughput of the compressor is 35%, which yields a compressed energy of 200 μJ. We expect to significantly enhance the low energy throughput with custom made and coated compressor components, which should result in throughput efficiencies of 60%–80% corresponding to up to 440 μJ pulse energy.

Upon compression, the temporal profile of the optical pulses was characterized using background-free intensity autocorrelation based on a ZGP crystal and all reflective optics. Figure 3 shows the measured trace, which exhibits an autocorrelation width of 360 fs. In order to evaluate the pulse duration, we fit various line shapes ($sech^2$, Gaussian, and Lorentzian) to the measured autocorrelation trace for its deconvolution. We find that the autocorrelation traces are best fitted with a Lorentzian temporal profile, which is sensible considering that pulse propagation suffers from residual absorption of small water content in the purged box, which would give rise to modification of the $sech^2$ autocorrelation profile in favor of a Lorentzian shape. Under this assumption, the AC trace corresponds to a pulse duration of 180 fs, which is shorter than eight optical cycles. As a comparison, the measured pulse duration would correspond to the same number of optical cycles as a 20-fs-duration pulse at the Ti:sapphire wavelength of 800 nm.

In order to leverage the full potential of the source to generate few-cycle pulses, advanced pulse diagnostics capabilities are warranted that can measure the pulse amplitude and phase at 7 μm rapidly. A straightforward implementation of methods such as FROG or SPIDER is, however, stymied by the absence of mid-IR array detectors with sufficient spatial or spectral resolution, thus resulting in unrealistically long scan times or insufficient resolution. We believe that methods such as electro-optical sampling will be ideally suited for direct and relatively fast waveform measurements in the mid-IR [35]. Further reduction in pulse duration should be straightforward to implement based on methods using spectral broadening and subsequent compression [36,37] or direct pulse compression in the mid-IR [38]. Last, we monitored the stability of the compressed output with a pyroelectric detector, and we measured an excellent system stability with energy fluctuations of less than 2.5% rms over 30 min (Fig. 4).

In conclusion, we have demonstrated, to the best of our knowledge, the first ultrafast mid-IR OPCPA directly operating at a center wavelength of 7 μm with a new OPCPA architecture leveraging nonoxide crystals that are directly pumped at 2 μm.

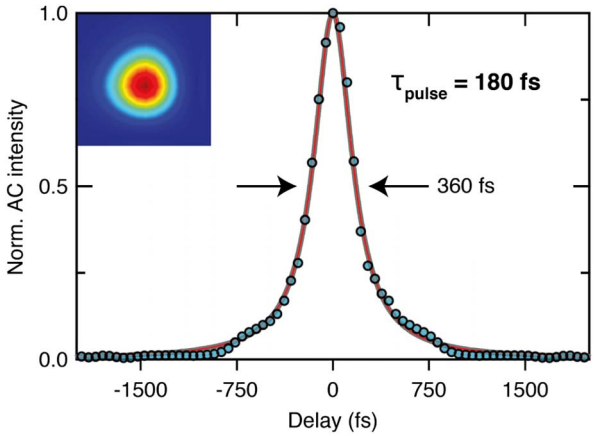

Fig. 3. Autocorrelation trace from a background-free intensity autocorrelation. Shown are the compressed pulses (blue circle) with the best-fitted pulse shape, which is a Lorentzian profile (solid red line). The deconvolution results in a pulse duration of 180 fs. Measured spatial profile (inset) of the compressed pulse at the output of the OPCPA.

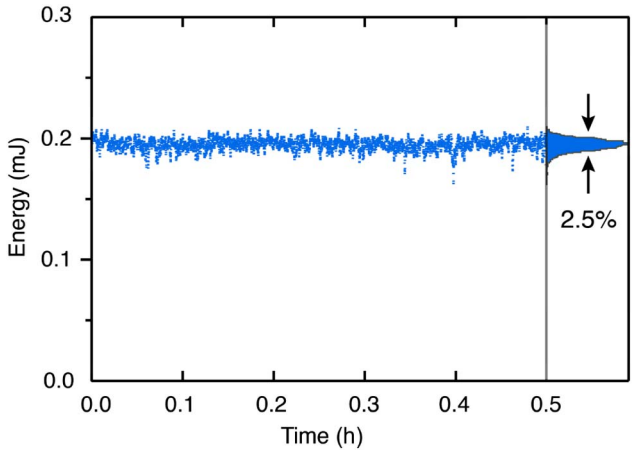

Fig. 4. Graph shows the OPCPA output pulse energy measured single shot and over a period of 30 min. We find excellent stability corresponding to 2.5% rms.

The entire system is fiber pumped and based on a multi-arm fiber front-end with different emission wavelengths, which provides the optical seed and optical synchronization without any electronics. The OPCPA seed is derived via DFG from two of those fiber outputs, which leads to a passively CEP-stable mid-IR frequency comb output at 100 MHz repetition rate. The pump laser is directly seeded by the same fiber front-end and consists of a Ho:YLF regenerative amplifier followed by a cryogenically cooled Ho:YLF single-pass amplifier. The 200 μJ output at 180 fs leads to a peak power of 1.1 GW and, if focused to the diffraction limit, to a peak intensity of 7×10^{14} W/cm^2, which is sufficient for strong-field experiments. Simulations indicate that the OPCPA architecture should be scalable to pump energies close to the joule level and to pulse energies in the tens of millijoule range at 7 μm. Further ongoing steps include increasing pulse energy through scaling of the Ho:YLF amplifier, careful tailoring of pump and seed pulse durations and chirp of the OPCPA stages, and further reduction of the pulse duration at 7 μm. We believe that the demonstrated pump and OPCPA architectures are attractive due to the compactness of the overall system and the fact that it is entirely fiber laser pumped, which reduces operating costs drastically. Moreover, the system's operating characteristics now enable access to the full mid-IR spectral range to ultrafast, nonlinear, and strong-field physics.

Funding. Spanish Ministry of Economy and Competitiveness (FIS2014-51478-ERC, FIS2014-56774-R); Severo Ochoa Programme for Centres of Excellence in R&D (SEV-2015-0522); Catalan Agencia de Gestió d'Ajuts Universitaris i de Recerca (AGAUR) (SGR 2014-2016); Fundació Cellex Barcelona; European Union's Horizon 2020 research and innovation programme Laserlab-Europe (654148); Marie Sklodowska-Curie (264666, 641272); German BMBF (E! 6698).

REFERENCES

1. S. Woutersen, U. Emmerichs, and H. J. Bakker, Science **278**, 658 (1997).
2. F. K. Tittel, D. Richter, and A. Fried, Top. Appl. Phys. **89**, 458 (2003).
3. B. Jean and T. Bende, Top. Appl. Phys. **89**, 530 (2003).
4. J. Reichert, R. Holzwarth, T. Udem, and T. W. Hänsch, Opt. Commun. **172**, 59 (1999).
5. S. A. Diddams, J. Opt. Soc. Am. B **27**, B51 (2010).
6. A. Schliesser, N. Picqué, and T. W. Hänsch, Nat. Photonics **6**, 440 (2012).
7. M. Hentschel, R. Kienberger, C. Spielmann, G. A. Reider, N. Milosevic, T. Brabec, P. Corkum, U. Heinzmann, M. Drescher, and F. Krausz, Nature **414**, 509 (2001).
8. J. Biegert, P. K. Bates, and O. Chalus, IEEE J. Sel. Top. Quantum Electron. Ultrafast Sci. Technol., invited review paper, **18**, 531 (2012).
9. J. Tate, T. Auguste, H. G. Muller, P. Salières, P. Agostini, and L. F. DiMauro, Phys. Rev. Lett. **98**, 013901 (2007).
10. T. Popmintchev, M. Chen, O. Cohen, M. Grisham, J. Rocca, M. Murnane, and H. Kapteyn, Opt. Lett. **33**, 2128 (2008).
11. M. V. Frolov, N. L. Manakov, and A. F. Starace, Phys. Rev. Lett. **100**, 173001 (2008).
12. S. L. Cousin, F. Silva, S. Teichmann, M. Hemmer, B. Buades, and J. Biegert, Opt. Lett. **39**, 5383 (2014).
13. F. Silva, S. Teichmann, S. L. Cousin, M. Hemmer, and J. Biegert, Nat. Commun. **6**, 6611 (2015).
14. F. Silva, P. K. Bates, A. Esteban-Martin, M. Ebrahim-Zadeh, and J. Biegert, Opt. Lett. **37**, 933 (2012).
15. P. Whalen, P. Panagiotopoulos, M. Kolesik, and J. V. Moloney, Phys. Rev. A **89**, 023850 (2014).
16. T. Auguste, P. Salières, A. S. Wyatt, A. Monmayrant, I. A. Walmsley, E. Cormier, A. Zaïr, M. Holler, A. Guandalini, F. Schapper, J. Biegert, L. Gallmann, and U. Keller, Phys. Rev. A **80**, 033817 (2009).
17. H. R. Reiss, Phys. Rev. Lett. **101**, 043002 (2008).
18. I. Jovanovic, G. Xy, and S. Wandel, Phys. Proc. **52**, 68 (2014).
19. O. Chalus, P. K. Bates, M. Smolarski, and J. Biegert, Opt. Express **17**, 3587 (2009).
20. H. Hoogland, A. Thai, D. Sanchez, S. L. Cousin, M. Hemmer, M. Engelbrecht, J. Biegert, and R. Holzwarth, Opt. Express **21**, 31390 (2013).
21. C. Erny, K. Moutzouris, J. Biegert, D. Kühlke, F. Adler, A. Leitenstorfer, and U. Keller, Opt. Lett. **32**, 1138 (2007).
22. A. Baltuska, T. Fuji, and T. Kobayashi, Phys. Rev. Lett. **88**, 133901 (2002).
23. T. Fuji, A. Apolonski, and F. Krausz, Opt. Lett. **29**, 632 (2004).
24. A. Thai, M. Hemmer, P. K. Bates, O. Chalus, and J. Biegert, Opt. Lett. **36**, 3918 (2011).
25. K. T. Zawilski, P. G. Schunemann, T. C. Pollak, D. E. Zelmon, N. C. Fernelius, and F. K. Hopkins, J. Cryst. Growth **312**, 1127 (2010).
26. D. Sánchez, M. Hemmer, M. Baudisch, K. Zawilski, P. Schunemann, H. Hoogland, R. Holzwarth, and J. Biegert, Opt. Lett. **39**, 6883 (2014).
27. B. W. Mayer, C. R. Phillips, L. Gallmann, and U. Keller, Opt. Express **22**, 20798 (2014).
28. G. Andriukaitis, T. Balciunas, S. Alisauskas, A. Pugzlys, A. Baltuska, T. Popmintchev, M. Chen, M. Murnane, and H. Kapteyn, Opt. Lett. **36**, 2755 (2011).
29. V. Petrov, Opt. Mater. **34**, 536 (2012).
30. P. Malevich, G. Andriukaitis, T. Flöry, A. J. Verhoef, A. Fernández, S. Ališauskas, A. Pugžlys, A. Baltuška, L. H. Tan, C. F. Chua, and P. B. Phua, Opt. Lett. **38**, 2746 (2013).
31. M. Hemmer, D. Sánchez, M. Jelínek, V. Smirnov, H. Jelinkova, V. Kubeček, and J. Biegert, Opt. Lett. **40**, 451 (2015).
32. L. von Grafenstein, M. Bock, U. Griebner, and T. Elsaesser, Opt. Express **23**, 14744 (2015).
33. H. Fonnum, E. Lippert, and M. W. Haakestad, Opt. Lett. **38**, 1884 (2013).
34. G. Arisholm, J. Opt. Soc. Am. B **14**, 2543 (1997).
35. I. Pupeza, D. Sánchez, J. Zhang, N. Lilienfein, M. Seidel, N. Karpowicz, T. Paasch-Colberg, I. Znakovskaya, M. Pescher, W. Schweinberger, V. Pervak, E. Fill, O. Pronin, Z. Wei, F. Krausz, A. Apolonski, and J. Biegert, Nat. Photonics **9**, 721 (2015).
36. M. Nisoli, S. De Silvestri, and O. Svelto, Appl. Phys. Lett. **68**, 2793 (1996).
37. T. Balciunas, C. Fourcade-Dutin, G. Fan, T. Witting, A. A. Voronin, A. M. Zheltikov, F. Gerome, G. G. Paulus, A. Baltuska, and F. Benabid, Nat. Commun. **6**, 6117 (2015).
38. M. Hemmer, M. Baudisch, A. Thai, A. Couairon, and J. Biegert, Opt. Express **21**, 28095 (2013).